The published version of the paper " F. Luzi, D. Puglia, F. Sarasini, J. Tirillò, G. Maffei, A. Zuorro, R. Lavecchia, J.M. Kenny, L.Torre (2019) Revalorization And Extraction Of Cellulose Nanocrystals From North African Grass: Ampelodesmos Mauritanicus (Diss) Carbohydrate Polymers, 209, 328-337" is available at: https://doi.org/10.1016/j.carbpol.2019.01.048

Revalorization And Extraction Of Cellulose Nanocrystals From North African Grass: *Ampelodesmos Mauritanicus* (*Diss*)

F. Luzi[a*], D. Puglia[a], F. Sarasini[b], J. Tirillò[b], G. Maffei[b], A. Zuorro[b], R. Lavecchia[b], J.M. Kenny[a], L. Torre[a]

[a]*University of Perugia, Civil and Environmental Engineering Department, UdR INSTM, Strada di Pentima 4, 05100 Terni, Italy*

[b]*Department of Chemical Engineering Materials Environment, Sapienza-Università di Roma, Via Eudossiana 18, 00184 Roma, Italy*

[*]**Corresponding author**: Francesca Luzi, Strada di Pentima 4, 05100 Terni (I), Tel.: +39-0744492914; fax: +39-0744492950; E-mail address: francesca.luzi@unipg.it.

Abstract

The aim of this research activity was based on the revalorization of *Amplodesmos Mauritanicus (Diss)*, an African grass largely presented in the Algerian territory. *Diss* stems were selected as native botanic material for the extraction of cellulose nanocrystals (CNC). Two different pretreatment steps were carried out to extract CNC from *Amplodesmos Mauritanicus* stems and the following acidic hydrolysis procedure allowed to extract/obtain cellulose nanocrystals in aqueous suspension. The effect of the two different pretreatments, based essentially on chemical or enzymatic treatments, were deeply investigated and the properties compared. Field emission scanning electron microscopy (FESEM), thermogravimetric analysis (TGA), Fourier transform infrared (FTIR) spectroscopy and X-ray diffraction (XRD) were considered for the characterization

of raw material, chemical or enzymatic treated *diss* stems and CNC extracted from both chemical and enzymatic pretreated cellulose.

Keywords: *Ampelodesmos mauritanicus*, cellulose nanocrystals, enzymatic treatment, acid hydrolysis.

1. Introduction

In the last few years, the revalorization of natural lignocellulosic material has promoted and induced the interest of academic research to consider this material as a valid alternative to the uncontrolled use of petroleum based materials in industrial applications. The ancient civilizations have utilized green fibres for over 40,000 years (Kvavadze et al., 2009) but, with the birth of industry and its development, people have started to design and use materials that are causing environmental problems in terms of greenhouse gas emissions (GHG) (F. Luzi, Fortunati, Jiménez, et al., 2016). In this context, the revalorization of agro and forest wastes is considered as a significant strategy to reduce the environmental impact, because their use could be fundamental for realization of new green products. The industrialization process has induced economic profits but, at the same time, highlighted some serious aspects that are affecting negatively the environment on a large scale, and the use of traditional materials, such as polymeric based products, is definitely implicated in this process. Over the last 15 years, this new perception has been also supported by environmental legislative pressures that established the GHG of different countries (Bourmaud, Beaugrand, Shaf, Placet, & Baley, 2018). In this framework, the revalorization of agro/forest wastes is also in the centre of politic interest because represents a valid strategy to increase the economic value of some countries.

Ampelodesmos mauritanicus is a large grass plant native of Northern Africa and Southern Europe and the dry regions of Greece and Spain, commonly known as Diss in Arabic, which belongs to the family of Poaceae (Toudert, Djilani, Djilani, Dicko, & Soulimani, 2009). This is a wild grass that grows spontaneously, with a chemical composition characterized by 44-46 % α-cellulose, 26-27 % hemicelluloses, 17-25 % lignin and 1.3 % fats and waxes, with a variable mineral content (SiO_2, Al_2O_3, Fe_2O_3, CaO, Na_2O and K_2O) (~ 8-10 %), depending on the plant development conditions, composition of the soil, and growth climatic conditions (Abdelhak, 2017; M. El H. Bourahli & Osmani, 2013; Chenah & Amrani, 2018). *Diss* plant has shown interesting mechanical and thermal properties (Achour, Ghomari, & Belayachi, 2017), thus promoting its use for the production of

traditional building materials in North Africa and artisanal baskets (Novellino, 2007). These fibres have been also used and largely studied for their interesting antiparasitic properties, which actually represent a traditional use of this plant (Toudert, Djilani, Djilani, et al., 2009). In the last years, it has been studied as potential biomass source for production of bioenergy, being these fibres characterized by low amount of fats and waxes (Gulias et al., 2018).

Toudert and co-authors proposed the study of flavonoids extracted from the aerial parts of *Ampelodesmos mauritanicus* and they observed antibacterial activity against gram positive bacteria and gram negative bacteria in vitro using the disc diffusion method. They detected the inhibition growth of *Escherichia coli* and *Staphylococcus saprophyticus*, while a reduced antimicrobial effect against *Pseudomonas aeruginosa* and *Staphylococcus epidermidis* was evidenced (Toudert, Djilani, & Djilani, 2009).

The chemical composition of plant fibres, which affects their properties, is related to their origin, age and type (Bledzki & Gassan, 1999). The most important components of plants are: lignin, hemicelluloses and cellulose. Lignin, an extremely crosslinked amorphous polymer (Sheltami, Abdullah, Ahmad, Dufresne, & Kargarzadeh, 2012) covers, encloses and protects the other two components, i.e. hemicelluloses and cellulose. Hemicellulose shows an amorphous structure, composed by repeated polymers of hexose and pentose units, which is also characterized by a branched multiple polysaccharide polymer (sugars: xylose, glucose, arabinose, mannose and galactose (Sheltami et al., 2012). Cellulose is responsible of mechanical strength and it is the main structural component of plant cell walls (Youssef Habibi, 2014). Cellulose is characterized by a linear syndiotactic and high-molecular weight homopolymer made up of β-d-glucopyranosyl units linked by 1–4 glycosidic bonds in different arrangements (He et al., 2018; Lu & Hsieh, 2010; Yang et al., 2018).

Furthermore, cellulose has been extensively studied as reinforcement phase at both micro and nano scale level in thermoplastic polymers for tuning some functional properties of the neat matrix (Arrieta, Peltzer, López, & Peponi, 2017; F. Luzi, Fortunati, Jiménez, et al., 2016; Puglia et al.,

2014; Shi et al., 2012). Cellulose nanocrystals can be extracted from different vegetable natural sources such as: (i) grass plants (okra, *Posidonia Oceanica,* etc.) (Bettaieb, Khiari, Hassan, et al., 2015; Fortunati et al., 2013, 2015; F. Luzi, Fortunati, Puglia, et al., 2016); (ii) annual plants (Phormium, Sunflowers, hemp, Kiwi, mengkuang leaves etc.) (Fortunati et al., 2014; Fortunati, Luzi, et al., 2016; Hanieh Kargarzadeh et al., 2012; F. Luzi et al., 2014; Francesca Luzi et al., 2017; Sheltami et al., 2012); (iii) agricultural waste (rice and barley husk, tomato peels, walnut shell and pistachio shells) (Fortunati, Benincasa, et al., 2016; Hemmati, Jafari, Kashaninejad, & Barani Motlagh, 2018; Jiang & Hsieh, 2015; Johar, Ahmad, & Dufresne, 2012; Kasiri & Fathi, 2018).

The final characteristics/properties and the geometric dimensions of cellulose nanocrystals (CNC) are directly dependent on the cellulosic native source, content of used fertilizers, soil characteristics (water content), agronomic and cultivar factors as plant maturity (F. Luzi et al., 2014). In addition, the preparation process and possible post-treatment after the CNC extraction influence the main characteristics of extracted cellulose nanocrystals (Fortunati et al., 2014; H. Kargarzadeh et al., 2018; F. Luzi et al., 2014). The main process for the isolation of cellulose nanocrystals from cellulose fibres is based on acid hydrolysis, in which disordered regions of cellulose are preferentially hydrolyzed, while crystalline regions, with higher resistance to acid attack, remain intact (Y Habibi, Lucia, & Rojas, 2010; Matos Ruiz, Cavaillé, Dufresne, Gérard, & Graillat, 2000; Neus Anglès & Dufresne, 2001). Sulfuric acid hydrolysis is the most common technique, because the resulting CNCs can be easily dispersed in water due to a small number of sulfate ester groups introduced to the surface of the CNCs during hydrolysis, whereas enzymatic, mechanical refining, and HCl hydrolysis leave the surface chemistry of the CNC unchanged (Sacui et al., 2014). All the common methodologies used to produce nanocellulose include different chemical steps to dissolve hemicelluloses and lignin from the lignocellulosic complex, in order to facilitate acid/enzymatic degradation. Therefore, new pretreatments are welcome to obtain nanocellulose with more environmentally friendly processes, making CNC a more attractive material for commercial exploitation.

The aim of this research activity was the extraction of cellulose nanocrystals from *Diss* stems that, to the best of authors' knowledge, has not been reported yet. Before the extraction of nanocellulose via an acid treatment, two different pretreatments, based essentially on chemical or enzymatic treatments, were applied to *Diss* stems and their effect on final yield and properties of nanofillers extracted by acid hydrolysis was studied. The raw material, the effects of different pretreatments (chemical or enzymatic) on *Diss* stems and the characteristics of CNC extracted from both chemical and enzymatic pretreated cellulose have been investigated by field emission scanning electron microscopy (FESEM), thermogravimetric analysis (TGA), Fourier transform infrared (FTIR) spectroscopy and X-ray diffraction (XRD).

2. Experimental section

2.1 Materials

Ampelodesmos Mauritanicus fibres, commonly called Diss, were collected from the north Mediterranean Africa in Batna in the east of Algeria (see visual image of Diss plant in **Figure 1**).

The enzymes Feedlyve AXC 1500L (AXC, principal component: β-1,4-xylanase), Peclyve EXVG (EXVG, principal component: Polygalacturonase) and Cellulyve 50LC (rich in cellulase) were provided by Lyven SA (Colombelles, France). The different chemical reagents were provided by Sigma Aldrich.

Abbreviation codes:

Diss: Diss stems;

C-treatment: chemically treated bleached *Diss* fibres;

E-treatment: enzymatically treated bleached *Diss* fibres;

C-CNC: Cellulose nanocrystals extracted from chemically treated bleached *Diss*;

E-CNC: Cellulose nanocrystals extracted from enzymatically treated bleached *Diss*.

2.2 Chemical pre-treatment of *Diss* fibres

Diss stems (visual image of Diss plant is shown in **Figure 1**) were washed several times in distilled water in order to remove soil contaminants and dust, then they were dried in an oven at 60°C for 24 h. The raw material was chopped into 5-10 mm elements and a de-waxing treatment in an ethanol/toluene mixture (1:2 volume/volume) for 6 h was carried out, followed by filtration and washing with ethanol for 30 min. Ethanol and toluene were used in a solution to remove the waxes from the raw material. The green colour of ethanol/toluene solution (visual image of ethanol/toluene solution is reported in **Figure 1**) was due to the fact that ethanol acted as a detergent/solvent, breaking down the phospholipid bilayer and opening holes in the membrane, making it permeable and promoting the elimination of the chloroplasts (Aires, Marbà, Serrao, Duarte, & Arnaud-Haond, 2012; F. Luzi, Fortunati, Puglia, et al., 2016). Two bleaching treatments were applied for cellulose extraction. At first the fibres were treated two times with a 0.7 % (wt/v) solution of sodium chlorite ($NaClO_2$), then were boiled for 2 h (fibre/liquor ratio 1:50). Sodium chlorite (puriss p.a. 80%) in aqueous solution was used as chemical treatment to bleach the fibres and to remove the lignin component. Thereafter, the pH of the solution was lowered to ca. 4, by adding acetic acid (CH_3COOH). Two bleaching treatments were necessary to obtain a complete whitening of the fibres. Then, a treatment with 5 % (wt/v) solution of sodium bisulphate ($NaHSO_4$) (F. Luzi et al., 2014) was carried out to extract holocellulose (α-cellulose + hemicellulose). The holocellulose was then treated with a 17.5 % (wt/v) solution of sodium hydroxide (reagent grade ≥ 98 %). NaOH aqueous treatment allowed to obtain α-cellulose component and to remove hemicelluloses. After filtration and washing, the obtained material was dried at 60°C in an air-circulating oven (**Figure 1** shows the visual image of C-treated material).

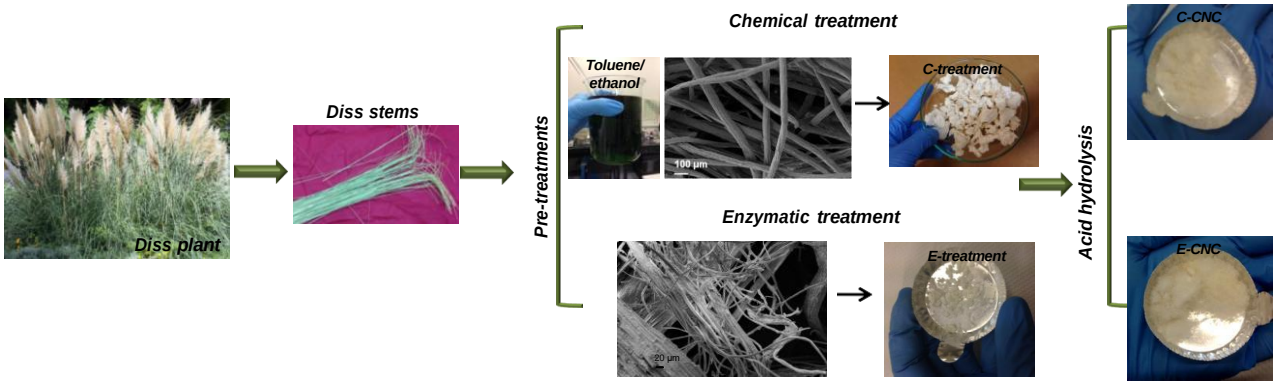

Figure 1: Visual image of *Diss* plant and stems. Scheme and image of *Diss* fibres during the chemical and enzymatic pre-treatment. Image of CNC powders after acid hydrolysis treatment applied to chemically and enzymatically bleached fibres.

2.3 Enzymatic pre-treatment

The enzymatic pre-treatment consisted of several steps. At first *Diss* stems were cut longitudinally in two parts (about 2 cm long) and were treated in an autoclave at 140°C for 1 h in a solution of KOH (0.25 M) with a liquid (mL) to solid (g) ratio of 20 mL/g. 1.5% (w/v) of $Na_2O_4S_2$ was added as reducing agent to protect cellulose. The pretreated fibres were washed several times with distilled water to remove KOH excess. Then a bleaching treatment followed, with a solution made of equal volumes of NaClO (1.7 wt%) and of a mixture at pH 4.5 (27g NaOH + 75ml CH_3COOH diluted in 1 L of distilled water) with a liquid (mL) to solid (g) ratio of 20 mL/g. The solution was treated in an autoclave at 125 °C for 2 h and then the solid part was washed several times with distilled water to remove solution excess. The enzymatic hydrolysis was performed in two separate steps. In the first step a mix of two commercial enzymatic formulations, one rich in xylanase (Feedlyve AXC) and one rich in pectinase (Peclyve EXG) was used. 50 mg/$g_{biomass}$ (25 mg of Peclyve EXG and 25

198 mg of Feedlyve AXC) in acetic acid/sodium acetate buffer at pH 5.25 with a liquid (mL) to solid (g)
199 ratio of 30 mL/g were added to the previous solution and placed in a thermostatic water bath at 50 ±
200 0.1 °C and magnetically stirred for 2 h. Once completed the hydrolysis, the samples have been
201 cooled down to room temperature. The suspension has been centrifuged at 7000 rpm for 5 minutes

and vacuum filtrated. This procedure has been repeated until a pH of 7 was reached. The second step has been performed by adding 100 $mg/g_{biomass}$ of a commercial enzymatic formulation rich in cellulase (Cellulyve 50LC) prepared in acetic acid/sodium acetate buffer at pH 4.5 with a liquid (mL) to solid (g) ratio of 30 mL/g. The sample was placed in a thermostatic water bath at 50 ± 0.1 °C and magnetically stirred for 15 h. Pre-treated fibres were then washed several times with distilled water to remove excess solution (**Figure 1** shows the visual image of E-treated material).

2.4 Cellulose nanocrystals

Cellulose nanocrystal (CNC) suspensions were prepared from chemically and enzymatically pre-treated cellulose by sulphuric acid hydrolysis (reagent 98%) (Fortunati et al., 2012) and the extracted CNCs were named C-CNC and E-CNC, respectively. The acid hydrolysis treatment enabled the dissolution of the amorphous region from bleached material and the extraction of cellulose nanocrystals. The hydrolysis was carried out with 64 % w/w sulphuric acid at 45 °C for 30 min with vigorous stirring. This reaction time was selected to guarantee the reaction efficiency and avoid crystal degradation. Immediately after the acid hydrolysis, the suspension was diluted 20 times with deionized water to quench the reaction. The suspension was centrifuged at 4.500 rpm for 20 min to concentrate the cellulose crystals and to remove the excess of aqueous acid. The resultant precipitate was rinsed, re-centrifuged, and dialyzed against deionized water for 5 days until constant neutral pH was achieved. The suspension was sonicated repeatedly (Vibracell 75043, 750W, Bioblock Scientific) at 40 % output (while cooled in an ice bath) to create cellulose crystals of colloidal dimensions.

2.5 Characterization of bleached fibres and cellulose nanocrystals

The thermal stability of raw material (*Diss*), bleached fibres (C-treatment and E-treatment) and extracted CNC (C-CNC and E-CNC) was evaluated by thermogravimetric analysis (TGA) using a

Setsys Evolution system by Setaram. All different cellulosic samples were heated from room temperature up to 800 °C in a nitrogen atmosphere with a heating rate of 10 °C min^{-1}.

Fourier infrared (FT-IR) spectra of raw material, chemically or enzymatically bleached fibres and cellulose nanocrystals extracted from chemically or enzymatically bleached materials were recorded using a Jasco FT-IR 615 spectrometer in the 400–4.000 cm^{-1} range, in transmission mode. The cellulosic materials were analyzed using KBr discs made by using pulverized natural materials and KBr powder.

The morphology of *Diss* and of pre-treated fibres was observed by scanning electron microscopy (SEM) using a Hitachi S-2500 and a Zeiss Auriga. All different specimens were sputter-coated with gold prior to analysis.

A morphological study of the obtained CNC based solution was also conducted by field emission scanning electron microscopy (FESEM, Supra 25-Zeiss). Few drops of CNC suspension, obtained after the hydrolysis procedure, were cast onto silicon substrate, vacuum dried and gold sputtered before the analysis.

The diameter of the fibres, the length and width of CNC were determined by using digital image analysis software (Nikon NIS-Elements BR). 100 duplicates have been recorded in order to obtain rational and reliable average values.

X-ray diffraction (XRD) analysis was performed at room temperature on a Philips X'Pert PRO powder diffractometer (CuK_α radiation = 1.54060 Å). XRD patterns were collected in the range of $2\theta = 10°–50°$ with a scan step $2\theta = 0.02°$ and a measurement time per step of 4 s.

The final yield after the hydrolysis process was calculated as % (of initial weight) of the used chemically or enzymatically treated fibres.

3. Results and Discussion

3.1 Analysis of chemical and enzymatic treatment of *Diss* fibres

3.1.1 Morphological investigation of Diss stems, chemically and enzymatically treated fibres

Figure 2 Panel A shows the morphology of *Diss* stems and *Diss* treated fibres (C-treated and E-treated), while **Figure 2 Panel B** displays the relative dimension of fibres (*Diss*, C-treated and E-treated).

Diss stems appeared as hollow and thin tubes (longitudinal observation, thickness in the range 300-450 μm, **Figure 2 Panel A, a)**): the longitudinal observation of *Diss* showed that the stems are composed by a high amount of fibres (dimension distribution d = (10.2 ± 2.2) μm **Figure 2 Panel B, a)**) all aligned in the same direction. The interconnection of different fibres in the stem can be correlated to the presence of lignin, hemicellulose and waxes. *Diss* structure is composed of cell element, vascular tissue and dermal tissue (Kennedy et al., 1999; Luzi, Fortunati, Puglia, et al., 2016; Sheltami et al., 2012). **Figure 2 Panel A, b)** shows the cross section of the stem, highlighting the internal structure and the arrangement of different cells. Specifically, the internal structure of *Diss* showed the presence of hollow tubes arranged in an honeycomb-like porous structure (Luzi et al., 2017; Sheltami et al., 2012).

The microstructural characteristics of chemically treated fibers are shown in **Figure 2 Panel A c) and d)**, while the morphological analysis of enzymatically treated fibres is reported in **Figure 2 Panel A e) and f)** at two different magnifications. It is possible to observe, in **Figure 2 Panel A** related to C-treatment and E-treatment, that both processes were able to reduce the cement components, as already reported in literature by Sheltami et al. (Sheltami et al., 2012). The treated fibres (C-treatment and E-treatment) appeared individualized with reduced diameter with respect to the values observed for *Diss* untreated fibres. Both procedures were able to remove waxes and ashes, lignin and hemicellulose components, as observed comparing the diameter frequency distribution of the different analyzed fibres (*Diss*, C-treated and E-treated) (**Figure 2 Panel B**). The treated fibres after the chemical and enzymatic treatment appeared completely white, as visible in the inset reported in **Figure 2 Panel B d) and f)**.

C-treated fibres showed a diameter mean value of (5.3 ± 1.1) μm, while the diameter mean value for E-treated was centred at around (4.9±1.5) μm. The treated fibres appeared with reduced diameter

with respect to *Diss* d = (10.2±2.2) μm, this effect underlined the efficiency of different applied procedures to remove lignin, hemicellulose and other components.

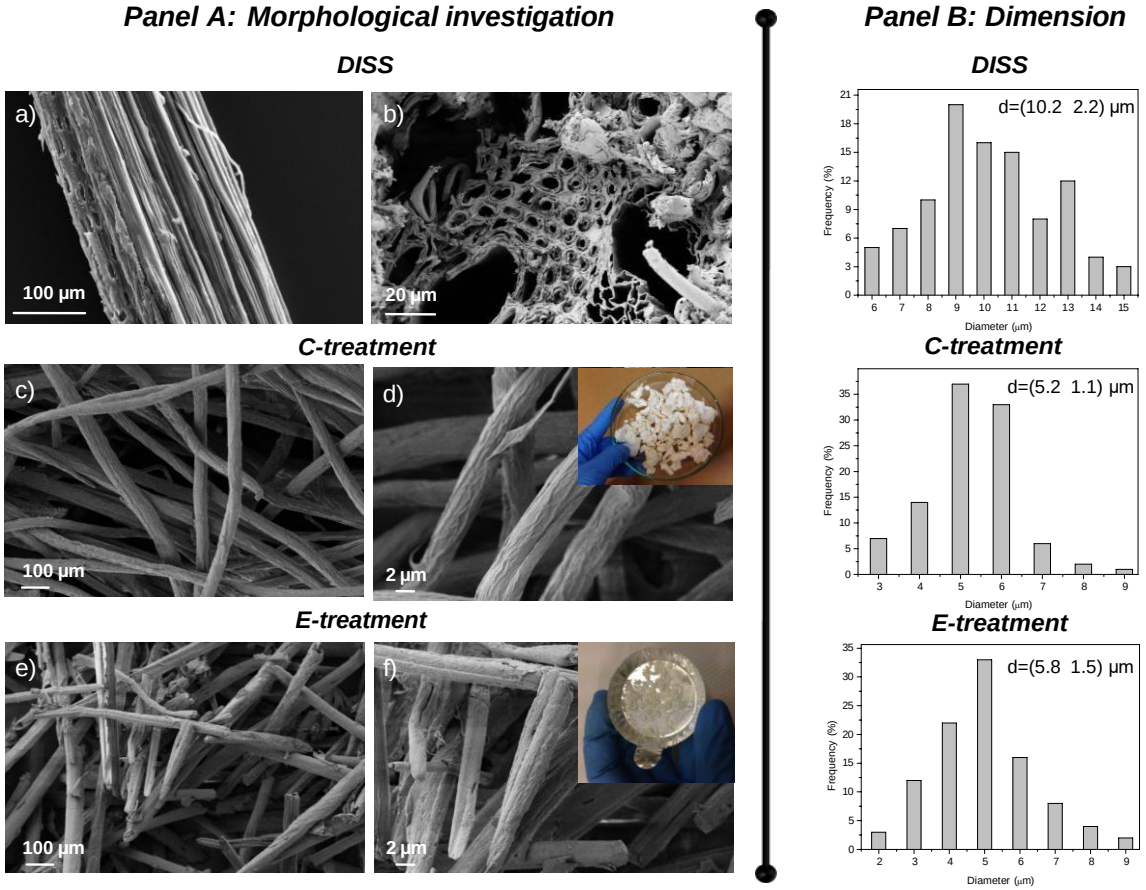

Figure 2: Panel A: Morphological characterization of *Diss* fibres: longitudinal **a)** and transversal section **b)**. FESEM investigation of bleached fibres applying chemical (**c)**) and **d)**) and enzymatic (**e)** and **f)** treatment at two different magnification. Visual image of treated fibers: **insert d)** chemically treated fibres and **insert f)** enzymatically treated fibres. **Panel B:** Diameter distributions of *Diss* **a)** and C-treated **b)** and E-treated **c)** fibres

3.1.2 Thermal analysis of Diss, chemically and enzymatically treated fibres

Thermal stability of Diss raw material, chemically and enzymatically treated fibres was investigated by thermogravimetric analysis (TGA).

Figure 3 shows the residual mass (TG, **Figure 3 a)**) and derivative (DTG, **Figure 3 b)**) curves for raw, chemically and enzymatically treated *Diss* fibres. In accordance with the literature, the

lignocellulosic materials showed a multistep degradative behaviour (El Achaby et al., 2017; Luzi, Fortunati, Puglia, et al., 2016; Silvério, Flauzino Neto, Dantas, & Pasquini, 2013). The presence of several degradation stages/steps indicated the presence of different components that are characterized by different temperatures of decomposition. The first thermal degradation step of *Diss*, C-treated and E-treated fibres was due to the presence of moisture/vaporization of water and volatile components that can be removed at a temperature below 150 °C (Lamaming et al., 2015; Mariano, El Kissi, & Dufresne, 2016; Puglia et al., 2014). The presence of water in the lignocellulosic fibres is ascribed to the higher hydrophilicity of these natural materials. The second peak of degradation at around 270 °C was attributed to hemicellulose degradation, which disappeared in treated fibres (C-treatment and E-treatment) (**Figure 3b**). The hemicellulose component degraded before lignin and cellulose, and its lower thermal stability is ascribed to the presence of acetyl groups (Hanieh Kargarzadeh et al., 2012). In the case of raw *Diss*, the third main peak of degradation was centred at around 320 °C, while for the treated fibres (cellulose fibres) C-treatment and E-treatment, it was located, respectively, at 347 °C and 350 °C.

The peak centred at 430 °C for raw material is related to the degradation of lignin component, as widely evidenced by existing literature (Pelissari, Sobral, & Menegalli, 2014; Nguyen, Zavarin, & barrall, 1981).

The residual mass, calculated at 800 °C, for raw *Diss*, C-treated and E-treated fibres, was also considered and reported in **Figure 3 b)**. The highest residual mass value was measured for *Diss* (30.9 % measured at 800 °C) (**Figure 3a)**), which is related to the presence of not degradable components at low temperatures, that were indeed removed after the treatments, with a more effective treatment in the case of enzymatic attack.

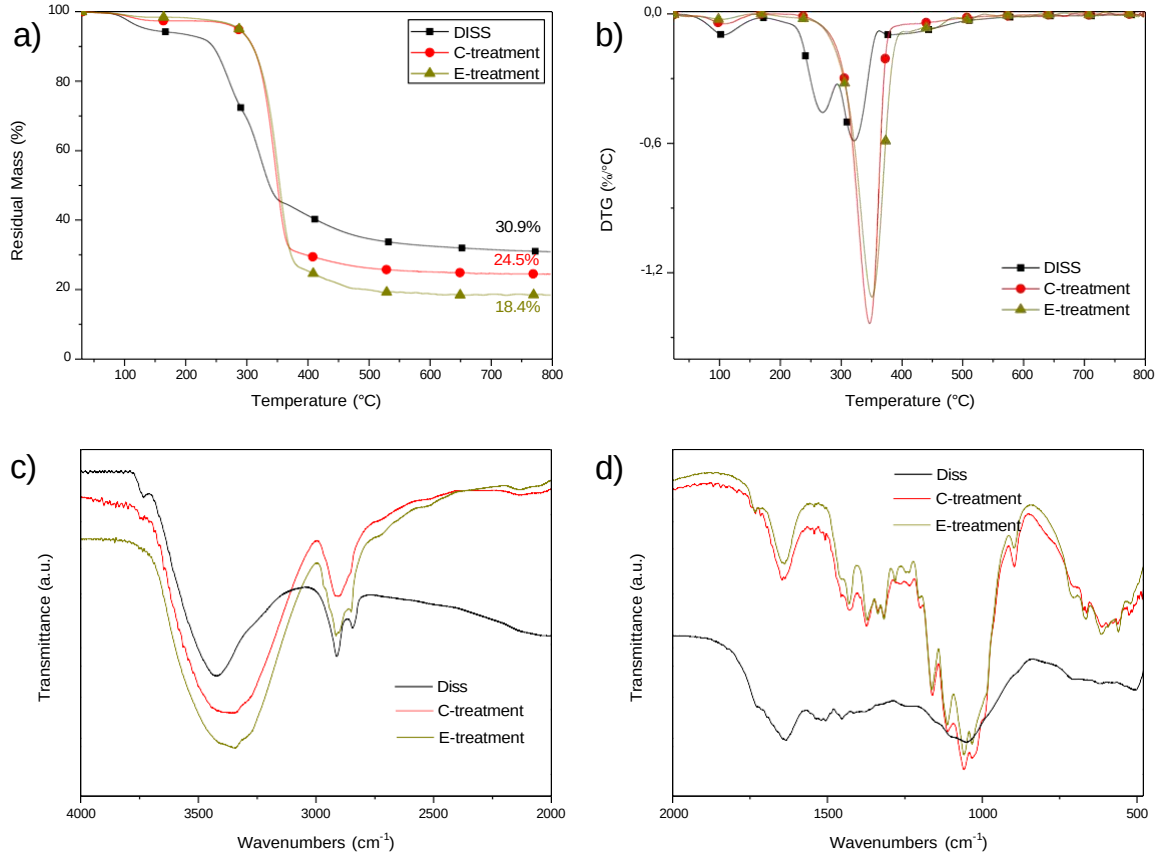

316

317 **Figure 3:** Residual mass (TG) **a)** and differential residual mass (DTG) **b)** curves of *Diss* and

318 bleached (C-treatment and E-treatment) fibres. FT-IR spectra of *Diss* and bleached (C-treatment

319 and E-treatment) fibres in the range of 4000-2000 cm^{-1} **a)** and 2000-400 cm^{-1} **b).**

320320

321 *3.1.3 FT-IR*

322 **Figures 3 c, d** show the FT-IR spectra of *Diss* and treated fibres (C-treated and E-treated) in two

323 different wavenumber ranges, from 4000 to 2000 cm^{-1} and from 2000 to 600 cm^{-1}, respectively.

324 The major absorbance peaks for untreated *Diss* fibres were observed at 3421 cm^{-1} reflecting the OH

325 groups, while the vibrations at 2911 and 2838 cm^{-1} correspond to saturated C–H stretching

326 vibrations from CH and CH_2 (**Figure 3, c)** (M. E. H. Bourahli, 2017). A band detected at 1731 cm^{-1}

327 corresponds to the carbonyl groups (C = O) of ester functions for hemicelluloses and lignin (Sain &

328 Panthapulakkal, 2006). The band at 1637 cm^{-1} is assigned to the β-glycosidic linkages between the

329 sugar units (Thomas & Owen, 1989), while the weak absorptions at 1523, 1455 and 1253 cm^{-1} arise

330 from the aromatic ring vibrations and C–O stretching of lignin. An intense band at 1045 cm^{-1}
331 corresponds to the C–O stretching modes of hydroxyl and ether groups (**Figure 3, d)**).
332 Finally, the broad band in the range 620 - 700 cm^{-1} might be associated with -CH- bond from
333 aromatic groups, as suggested by Bessadok et al. (Bessadok et al., 2007).
334 In the case of chemically treated *Diss* fibres (C-treated), the different intensity of the C-H stretching
335 vibration at 2900 cm^{-1} can be considered as a measure of the general organic material content of the
336 fibre (**Figure 3, c)**). The prominent peak at 1731 cm^{-1} disappeared completely, indicating the
337 removal of most of the lignin and hemicelluloses (Chen et al., 2011). The spectral band at 1648
338 cm^{-1} is due to OH bending of adsorbed water, while the peak at 1367 cm^{-1} is due to the COH
339 stretching of the hydrogen bond of crystalline cellulose. The band at 1315 cm^{-1} corresponds to –
340 CH_2– wagging of cellulose. The C-C ring breathing band at 1159 cm^{-1} and the C-O-C glycosidic
341 ether band at 1107 cm^{-1} arise from the polysaccharide component (Garside & Wyeth, 2003), while
342 the peak at 1061 cm^{-1}, due to the shift of the original 1045 cm^{-1} related to the xylane and the
343 glycosidic linkages of hemicellulose, was detected, proving the removal of hemicellulose after
344 treatment. Vibration of functional groups C-H and stretching of C-O group also appeared at 1029
345 cm^{-1} for bleached *Diss* (Johar et al., 2012) (**Figure 3, d)**). The peak observed at 894 cm^{-1} indicates
346 the presence of the cellulosic glycosidic linkages between the monosaccharides (Kabir, Wang, Lau,
347 & Cardona, 2013).
348 In the case of enzymatic pretreatment (E-treated), the direct comparison with the spectrum of C-
349 treated Diss indicated a general superposition of the significant vibrations, with few deviations in
350 terms of intensity: the bending vibration of (-OH), due to physically absorbed water, was detected at
351 1637 cm^{-1}, while the presence of a vibration at 1736 cm^{-1}, being characteristic for unconjugated
352 carbonyl groups (C=O), as well as a band at 1246 cm^{-1}, which is associated to the acetyl group, are
353 representative of partial removal of hemicellulose component (Abidi, Cabrales, & Haigler, 2014)
354 (**Figure 3, d)**). Peaks corresponding to cellulose (1318 cm^{-1} and 1372 cm^{-1}) showed higher
355 intensity (Li & Pickering, 2008), while peaks at 1453, 1162 and 1112 cm^{-1}, assigned to the C-O-C

and C-O stretching vibration of lignin (in alcohols), still showed relatively higher intensity after the enzymatic treatment (**Figure 3, d)**). Even the presence of more intense peaks at 1278, 1247 and 1236 cm^{-1} indicated the persistent presence of lignin fractions (Saliba, Rodriguez, Morais, & Piló-Veloso, 2001). Other signals can be found at 1337 $cm^{-1}$and 990 cm^{-1}, representative of H-O-C bending in cellulose and hemicelluloses, respectively (**Figure 3, d)**).

3.2 Investigation of cellulose nanocrystals extracted from chemically and enzymatically treated fibres

3.2.1 Morphological investigation of CNC

Figure 4 Panel A shows the FESEM investigation of CNC obtained by applying the acid hydrolysis treatment to chemically (**Figure 4 Panel A, a))** and enzymatically (**Figure 4 Panel A, b)** treated fibres, while the **Figure 4 Panel B** summarizes the dimension's frequency (diameter and length) of C-CNC and E-CNC.

FESEM images (**Figure 4 Panel A, a-b)**) show isolated and individual nanostructures with the typical acicular and needle-like morphology of cellulose nanocrystals, as already observed in literature for other nanocrystals extracted from several natural fibres (Bettaieb, Khiari, Dufresne, Mhenni, & Belgacem, 2015; El Achaby et al., 2017; Fortunati et al., 2014; Kumar, Negi, Choudhary, & Bhardwaj, 2014; F. Luzi, Fortunati, Puglia, et al., 2016; Francesca Luzi et al., 2017).

A reaction efficiency of the acid hydrolysis for both cellulose nanocrystals was estimated at around 8.7 % and 8.3 % for C-CNC and E-CNC, respectively. Differences in terms of shape were observed for C-CNC and E-CNC (**Figure 4 Panel A, a-b)**): C-CNC are characterized by reduced size compared to E-CNC, in particular C-CNC showed a diameter and length mean values of (21.2 ± 5.1) nm and (180 ± 40) nm, respectively, while the E-CNC showed a diameter and length mean values of (32.7 ± 5.5) nm and (238 ± 34) nm, respectively.

The obtained results about CNC dimensions confirmed that the final characteristics/properties and the geometric dimensions of cellulose nanocrystals are not only directly dependent on the cellulosic

native source (F. Luzi et al., 2014), but also on the extraction process and possible pre-treatments of CNC can influence the principal characteristics of extracted cellulosic nanostructures (Fortunati et al., 2014; H. Kargarzadeh et al., 2018; F. Luzi et al., 2014).

The morphologies observed for nanocelluloses isolated from *Diss*, by simply varying the pre-processing conditions, and the heterogeneity in size observed for these CNCs demonstrate the diffusion controlled nature of acid hydrolysis (Sacui et al., 2014).

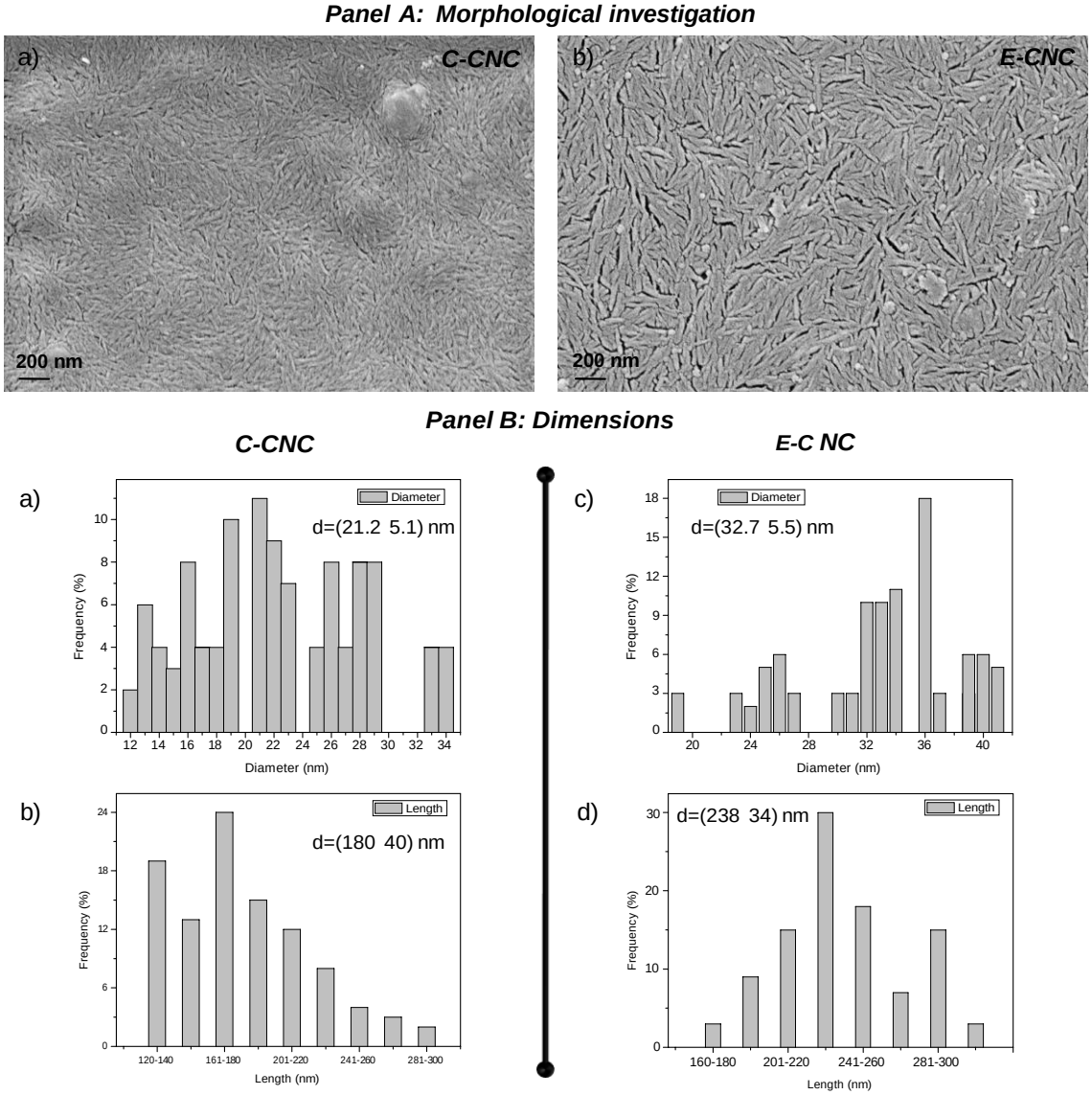

Figure 4: Panel A: Morphological characterization of cellulose nanocrystals extracted applying acid hydrolysis procedure to chemically **a)** and enzymatically **b)** treated fibres. Diameter and length

distributions of C-CNC (**c)** and d**)**, respectively) E-CNC (e**)** and f**)**, respectively). **Panel B**: cellulose nanocrystal dimensions (diameter and length) of C-CNC (**a)** and **b)**) and E-CNC (**c)** and **d)**).

3.2.2 CNC thermal analysis

Thermal degradative behaviour of cellulose nanocrystals (C-CNC and E-CNC) was analysed by thermogravimetric analysis (TGA).

Generally, CNC thermal degradation occurs at a lower temperature compared to raw materials within broader ranges of temperature. The lower thermal stability of CNC with respect to the native material is due to their nanodimensions and is triggered by degradation of sulphated amorphous regions and reduction in molecular weight (Kumar et al., 2014; Mandal & Chakrabarty, 2011). **Figure 5** shows the derivative curves of the mass loss (DTG, **Figure 5 a)**) for both CNCs. The degradation of CNC is characterized by multistep degradative trend which is consistent with the literature (Fortunati, Luzi, et al., 2016; Lamaming et al., 2015; Mariano et al., 2016).

The first thermal degradation of CNC is due to the presence of moisture that can be removed at a temperature lower than 150 °C, as reported elsewhere (Lamaming et al., 2015; Mariano et al., 2016; Puglia et al., 2014).

The main pyrolysis process of C-CNC and E-CNC is characterized by two degradation peaks centred at around 285 °C and 343 °C for C-CNC and 295 °C and 353 °C for E-CNC. The first peak is due to the weaker interaction of single bond OH group in cellulosic component, that requires less energy during the degradation process, while the second degradative peak can be correlated to packed and ordered cellulose regions, higher crystalline domains/crystal dimensions, therefore high stability. The surface sulphated groups lower the degradation temperature of CNCs, specifically in the case of C-CNC: the elimination of sulphuric acid in sulphated anhydroglucose units required less energy with respect of E-CNC, and thus they could be released at much lower temperatures

during the thermal degradation process. More importantly, among these two different CNCs, E-

CNC exhibited the highest stability, benefiting from less damage in the crystalline regions (Yu et al., 2013).

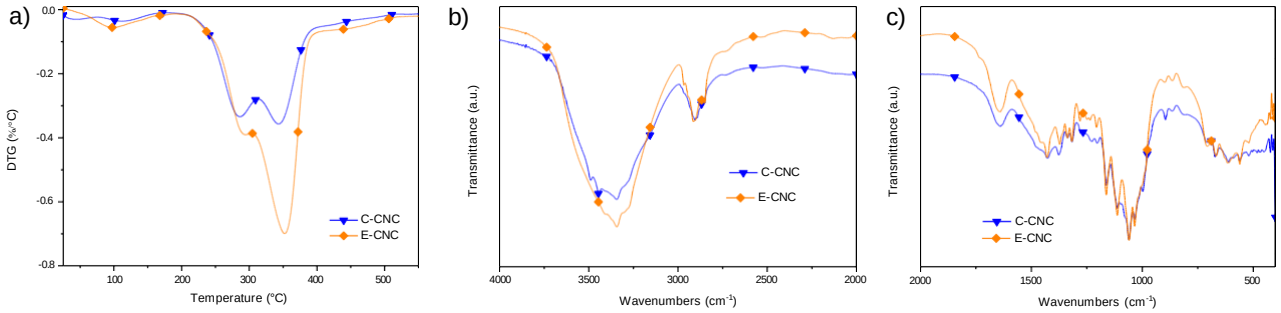

Figure 5: Residual mass (TG) **a)** and differential residual mass (DTG) **b)** curves of CNC (C-CNC and E-CNC). FT-IR spectra of CNC (C-CNC and E-CNC) in the ranges of 4000-400 cm^{-1} **c)** and in the range 2000-400 cm^{-1} **d)**.

3.2.3 FT-IR

Figures 5 b, c show the FT-IR spectra of cellulose nanocrystals in two different wavenumber ranges, from 4000 to 2000 cm^{-1} and from 2000 to 600 cm^{-1}, respectively.

The spectrum of cellulose nanocrystals extracted by chemical bleaching (C-CNC) revealed common and easily identifiable bands as, for example, adsorbed water in cellulose (1637 cm^{-1}), and bands at 1424, 1478, 1378, 1336 and 1320 cm^{-1} attributed to CH_2 symmetric bending, CH bending, in-plane OH bending, CH_2 rocking vibration, respectively (H. Chen et al., 2010) (**Figure 5, c)**). Furthermore, the signals at 1159, 1107, 1060, 1035, 894 cm^{-1} are assigned to asymmetric COC bridge stretching, anhydroglucose ring asymmetric stretching, CO stretching, in-plane CH deformation and CH deformation of cellulose, respectively (Corgié, Smith, & Walker, 2011). The peak at 997 cm^{-1} is due to the transformation from cellulose I to cellulose II (Gwon, Lee, Doh, & Kim, 2010), while the selected signal at 671 cm^{-1} is due to C-OH out-of-phase bending (Fan, Dai, & Huang, 2012).

In the case of CNC extracted from enzymatic pretreatment (E-CNC) (**Figure 5, c)**), several common characteristic peaks are found: the peak at 1637 cm^{-1} can be attributed to the OH bending

of the absorbed water, while the vibration peak detected at 1428, 1373, 1336 and 1317 cm^{-1}, respectively related to the CH_2, CH, CO and in-plane OH bending vibration in the polysaccharide aromatic rings showed higher intensity. The peak observed at 1060 cm^{-1} (COC pyranose ring skeletal vibration) was more evident, while the signals at 894 and 863 cm^{-1}, which correspond to glycosidic CH deformation, are essentially comparable with the ones visible in C-CNC (**Figure 5, c)**) (Alemdar & Sain, 2008).

3.3 XRD

The X-ray diffraction patterns of *Diss*, treated fibres (C-treatment and E-treatment) and cellulose nanocrystals (C-CNC and E-CNC) are shown in **Figure 6**. The XRD analysis was performed to evaluate the crystalline structure at different chemical and enzymatic treatments.

The main characteristic peaks of raw *Diss* were located at 2Θ= 16.4°, 22.6°, and 35.4°, these peaks are assigned to cellulose I (Kasiri & Fathi, 2018; Thambiraj & Ravi Shankaran, 2017) and appeared in all samples. Peak at 2Θ = 16.4° corresponds to (110) plane, while 2Θ = 22.6° and 2Θ = 35.4° are characteristic peaks of (002) and (004) planes, respectively.

XRD patterns for all cellulosic materials showed the main peak at around 22.6°, with a slight shift was detected for C-treatment at 2Θ = 22.2°, E-treatment at 2Θ = 22.4° and C-CNC at 2Θ = 22.2°, due to different applied treatments and consistent with the literature (Fortunati, Benincasa, et al., 2016). The plane (002) that corresponds to the peak centred at around 2Θ =22.6° indicated, in cellulose I domains, the distance between hydrogen bonded sheets.

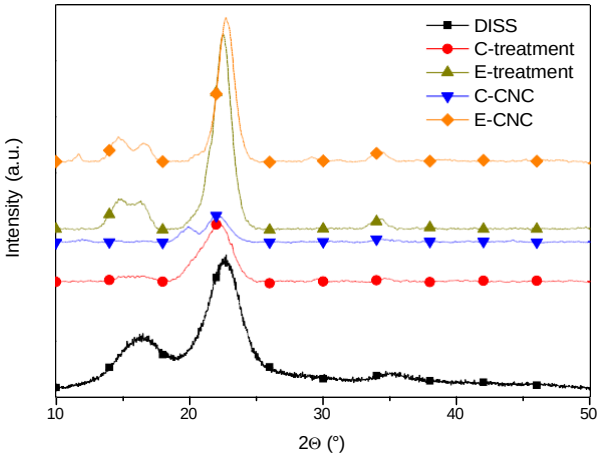

Figure 6: XRD patterns of *Diss*, pretreated (C-treated and E-treated) fibres and CNC (C-CNC and E-CNC) obtained applying acid hydrolysis treatment to chemical and enzymatic treatment treated fibres.

After the chemical, enzymatic and acid treatments the (1-10) plane (2Θ = 14.7°) appeared to be separated from the plane (101) (2Θ = 16.4°), which are also typical of cellulose I (Fortunati, Benincasa, et al., 2016; Thambiraj & Ravi Shankaran, 2017). The peaks at 14.8°, 16.6° and at 34.5° are typical peaks of cellulose I; they are related to the alignment of chains into the fibrils and of the order along the fibre direction (Besbes, Alila, & Boufi, 2011).

Enzymatic treatment resulted in major changes in X-ray diffraction patterns. The typical cellulose pattern, already observed for CNC extracted from chemically treated fibres, shows additional well-defined peaks at 29.4° and 35.8°. These diffraction peaks, which correspond to very short atomic interactions, may be tentatively ascribed to the formation of new crystalline domains likely originated from the enzymatic degradation of cellulose I or amorphous cellulose. In fact, the enzymatic treatment might depolymerize the cellulose macromolecules with the formation of

shorter chains able to form denser crystalline domains (F. Luzi et al., 2014).

4. Conclusions

Extraction of cellulose nanocrystals has been successfully carried out from *Diss* stems. *Diss* stems were pre-treated by considering chemical (bleaching) and enzymatic treatments (combined action of xylase, pectinase and cellulose enzymes). The effect of different pre-treatments on thermal, chemical and structural characteristics of the extracted cellulosic fibres was analyzed and compared. Morphological investigation of treated fibres showed that both treatments acted positively towards the reduction of fiber diameter size, underlining how the different treatments were both able to eliminate no cellulosic components. FESEM analysis of C-CNC and E-CNC also confirmed that both procedures, in combination with the acidic treatment, are able to extract CNC at nanoscale level. Results of X-ray diffraction measurements showed the presence, in the case of CNC extracted from enzymatically treated fibers, of additional well-defined peaks, in comparison to CNC extracted from chemically treated fibers, ascribed to the formation of new crystalline domains originated from the enzymatic degradation of cellulose I. These findings well correlated with the improved thermal stability of E-CNC.

Differences in terms of shape were observed for C-CNC and E-CNC. C-CNC are characterized by reduced size compared to E-CNC, in particular C-CNC showed diameter and length mean values of (21.2 ± 5.1) nm and (180 ± 40) nm, respectively, while the E-CNC showed diameter and length mean values of (32.7 ± 5.5) nm and (238 ± 34) nm, confirming how final characteristics/properties and geometric dimensions of cellulose nanocrystals are not only directly dependent on native source, but also on extraction and pre-treatments methods, strictly correlated to the diffusion controlled nature of acid hydrolysis. The thermal, chemical and morphological characteristics of the cellulose nanocrystals extracted from *Diss* stems could be of interest in a nanocomposite approach, in which CNC could be considered as reinforcement phase at the nanoscale level. The results indicate that the use of *Diss*, namely an attractive feedstock that can grow on less fertile or marginal lands, requiring modest pest and disease management, can be exploited in various fields where high value added products are demanded.

References

Abdelhak, M. (2017). Study of Some North African Grasses (Ampelodesma mauritanica and Esparto Grass). In *Grasses - Benefits, Diversities and Functional Roles*. InTech. http://doi.org/10.5772/intechopen.70001

Abidi, N., Cabrales, L., & Haigler, C. H. (2014). Changes in the cell wall and cellulose content of developing cotton fibers investigated by FTIR spectroscopy. *Carbohydrate Polymers*, *100*, 9–16. http://doi.org/10.1016/J.CARBPOL.2013.01.074

Achour, A., Ghomari, F., & Belayachi, N. (2017). Properties of cementitious mortars reinforced with natural fibers. *Journal of Adhesion Science and Technology*, *31*(17), 1938–1962. http://doi.org/10.1080/01694243.2017.1290572

Aires, T., Marbà, N., Serrao, E. A., Duarte, C. M., & Arnaud-Haond, S. (2012). Selective elimination of chloroplastidial DNA for Metagenomics of bacteria associated with the green alga caulerpa taxifolia (BRYOPSIDOPHYCEAE). *Journal of Phycology*, *48*(2), 483–490. http://doi.org/10.1111/j.1529-8817.2012.01124.x

Alemdar, A., & Sain, M. (2008). Biocomposites from wheat straw nanofibers: Morphology, thermal and mechanical properties. *Composites Science and Technology*, *68*(2), 557–565. http://doi.org/10.1016/J.COMPSCITECH.2007.05.044

Arrieta, M. P., Peltzer, M. A., López, J., & Peponi, L. (2017). PLA-Based Nanocomposites Reinforced with CNC for Food Packaging Applications: From Synthesis to Biodegradation. In *Industrial Applications of Renewable Biomass Products* (pp. 265–300). Cham: Springer International Publishing. http://doi.org/10.1007/978-3-319-61288-1_11

Besbes, I., Alila, S., & Boufi, S. (2011). Nanofibrillated cellulose from TEMPO-oxidized eucalyptus fibres: Effect of the carboxyl content. *Carbohydrate Polymers*, *84*(3), 975–983. http://doi.org/10.1016/J.CARBPOL.2010.12.052

Bessadok, A., Marais, S., Gouanvé, F., Colasse, L., Zimmerlin, I., Roudesli, S., & Métayer, M. (2007). Effect of chemical treatments of Alfa (Stipa tenacissima) fibres on water-sorption properties. *Composites Science and Technology*, *67*(3–4), 685–697. http://doi.org/10.1016/J.COMPSCITECH.2006.04.013

Bettaieb, F., Khiari, R., Dufresne, A., Mhenni, M. F., & Belgacem, M. N. (2015). Mechanical and thermal properties of Posidonia oceanica cellulose nanocrystal reinforced polymer. *Carbohydrate Polymers*, *123*, 99–104. http://doi.org/10.1016/j.carbpol.2015.01.026

Bettaieb, F., Khiari, R., Hassan, M. L., Belgacem, M. N., Bras, J., Dufresne, A., & Mhenni, M. F. (2015). Preparation and characterization of new cellulose nanocrystals from marine biomass Posidoniaoceanica. *Industrial Crops and Products*, *72*, 175–182. http://doi.org/10.1016/J.INDCROP.2014.12.038

Bledzki, A., & Gassan, J. (1999). Composites reinforced with cellulose based fibres. *Progress in Polymer Science*, *24*, 221–274. Retrieved from http://www.sciencedirect.com/science/article/pii/S0079670098000185

Bourahli, M. E. H. (2017). Uni- and bimodal Weibull distribution for analyzing the tensile strength of Diss fibers. *Journal of Natural Fibers*, 1–10. http://doi.org/10.1080/15440478.2017.1371094

Bourahli, M. E. H., & Osmani, H. (2013). Chemical and Mechanical Properties of Diss (*Ampelodesmos mauritanicus*) Fibers. *Journal of Natural Fibers*, *10*(3), 219–232. http://doi.org/10.1080/15440478.2012.761115

Bourmaud, A., Beaugrand, J., Shaf, D. U., Placet, V., & Baley, C. (2018). Towards the design of high-performance plant fibre composites. *Progress in Materials Science*, *97*, 347–408. http://doi.org/10.1016/J.PMATSCI.2018.05.005

Chen, H., Ferrari, C., Angiuli, M., Yao, J., Raspi, C., & Bramanti, E. (2010). Qualitative and quantitative analysis of wood samples by Fourier transform infrared spectroscopy and multivariate analysis. *Carbohydrate Polymers*, *82*(3), 772–778.

554 http://doi.org/10.1016/J.CARBPOL.2010.05.052
555 Chen, W., Yu, H., Liu, Y., Chen, P., Zhang, M., & Hai, Y. (2011). Individualization of cellulose
556 nanofibers from wood using high-intensity ultrasonication combined with chemical
557 pretreatments. *Carbohydrate Polymers*, *83*(4), 1804–1811.
558 http://doi.org/10.1016/J.CARBPOL.2010.10.040
559 Chenah, M., & Amrani, M. (2018). Physical and Chemical Characterization of Ampelodesmos
560 Mauritanicus. In *Recent Advances in Environmental Science from the Euro-Mediterranean and*
561 *Surrounding Regions. EMCEI 2017* (pp. 1235–1236). Springer, Cham.
562 http://doi.org/10.1007/978-3-319-70548-4_357
563 Corgié, S. C., Smith, H. M., & Walker, L. P. (2011). Enzymatic transformations of cellulose
564 assessed by quantitative high-throughput fourier transform infrared spectroscopy (QHT-FTIR).
565 *Biotechnology and Bioengineering*, *108*(7), 1509–1520. http://doi.org/10.1002/bit.23098
566 El Achaby, M., El Miri, N., Aboulkas, A., Zahouily, M., Bilal, E., Barakat, A., & Solhy, A. (2017).
567 Processing and properties of eco-friendly bio-nanocomposite films filled with cellulose
568 nanocrystals from sugarcane bagasse. *International Journal of Biological Macromolecules*, *96*,
569 340–352. http://doi.org/10.1016/j.ijbiomac.2016.12.040
570 Fan, M., Dai, D., & Huang, B. (2012). Fourier Transform Infrared Spectroscopy for Natural Fibres.
571 In *Fourier Transform - Materials Analysis*. InTech. http://doi.org/10.5772/35482
572 Fortunati, E., Armentano, I., Zhou, Q., Iannoni, A., Saino, E., Visai, L., Kenny, J. M. (2012).
573 Multifunctional bionanocomposite films of poly(lactic acid), cellulose nanocrystals and silver
574 nanoparticles. *Carbohydrate Polymers*, *87*(2), 1596–1605.
575 http://doi.org/10.1016/j.carbpol.2011.09.066
576 Fortunati, E., Benincasa, P., Balestra, G. M., Luzi, F., Mazzaglia, A., Del Buono, D., … Torre, L.
577 (2016). Revalorization of barley straw and husk as precursors for cellulose nanocrystals
578 extraction and their effect on PVA_CH nanocomposites. *Industrial Crops and Products*, *92*,
579 201–217. http://doi.org/10.1016/J.INDCROP.2016.07.047
580 Fortunati, E., Luzi, F., Jiménez, A., Gopakumar, D. A., Puglia, D., Thomas, S., … Torre, L. (2016).
581 Revalorization of sunflower stalks as novel sources of cellulose nanofibrils and nanocrystals
582 and their effect on wheat gluten bionanocomposite properties. *Carbohydrate Polymers*, *149*,
583 357–368. http://doi.org/10.1016/J.CARBPOL.2016.04.120
584 Fortunati, E., Luzi, F., Puglia, D., Dominici, F., Santulli, C., Kenny, J. M., & Torre, L. (2014).
585 Investigation of thermo-mechanical, chemical and degradative properties of PLA-limonene
586 films reinforced with cellulose nanocrystals extracted from Phormium tenax leaves. *European*
587 *Polymer Journal*, *56*, 77–91. http://doi.org/10.1016/J.EURPOLYMJ.2014.03.030
588 Fortunati, E., Luzi, F., Puglia, D., Petrucci, R., Kenny, J. M., & Torre, L. (2015). Processing of
589 PLA nanocomposites with cellulose nanocrystals extracted from Posidonia oceanica waste:
590 Innovative reuse of coastal plant. *Industrial Crops and Products*, *67*, 439–447.
591 http://doi.org/10.1016/j.indcrop.2015.01.075
592 Fortunati, E., Puglia, D., Monti, M., Santulli, C., Maniruzzaman, M., & Kenny, J. M. (2013).
593 Cellulose nanocrystals extracted from okra fibers in PVA nanocomposites. *Journal of Applied*
594 *Polymer Science*, *128*(5), 3220–3230. http://doi.org/10.1002/app.38524
595 Garside, P., & Wyeth, P. (2003). Identification of Cellulosic Fibres by FTIR Spectroscopy - Thread
596 and Single Fibre Analysis by Attenuated Total Reflectance. *Studies in Conservation*, *48*(4),
597 269–275. http://doi.org/10.1179/sic.2003.48.4.269
598 Gulias, J., Melis, R., Scordia, D., Cifre, J., Testa, G., Cosentino, S. L., & Porqueddu, C. (2018).
599 Exploring the potential of wild perennial grasses as a biomass source in semi-arid
600 Mediterranean environments. *Italian Journal of Agronomy*, 103–111.
601 http://doi.org/10.4081/ija.2018.937
602 Gwon, J. G., Lee, S. Y., Doh, G. H., & Kim, J. H. (2010). Characterization of chemically modified
603 wood fibers using FTIR spectroscopy for biocomposites. *Journal of Applied Polymer Science*,
604 *116*(6), NA-NA. http://doi.org/10.1002/app.31746

Habibi, Y. (2014). Key advances in the chemical modification of nanocelluloses. *Chemical Society Reviews*, *43*(5), 1519–42. http://doi.org/10.1039/c3cs60204d

Habibi, Y., Lucia, L., & Rojas, O. (2010). Cellulose nanocrystals: Chemistry, selfassembling, and applications. *Chemical Reviews*, *110*(3479–3500).

He, X., Luzi, F., Yang, W., Xiao, Z., Torre, L., Xie, Y., & Puglia, D. (2018). Citric Acid as Green Modifier for Tuned Hydrophilicity of Surface Modified Cellulose and Lignin Nanoparticles. *ACS Sustainable Chemistry & Engineering*, *6*(8), 9966–9978. http://doi.org/10.1021/acssuschemeng.8b01202

Hemmati, F., Jafari, S. M., Kashaninejad, M., & Barani Motlagh, M. (2018). Synthesis and characterization of cellulose nanocrystals derived from walnut shell agricultural residues. *International Journal of Biological Macromolecules*, *120*, 1216–1224. http://doi.org/10.1016/J.IJBIOMAC.2018.09.012

Jiang, F., & Hsieh, Y.-L. (2015). Cellulose nanocrystal isolation from tomato peels and assembled nanofibers. *Carbohydrate Polymers*, *122*, 60–68. http://doi.org/10.1016/J.CARBPOL.2014.12.064

Johar, N., Ahmad, I., & Dufresne, A. (2012). Extraction, preparation and characterization of cellulose fibres and nanocrystals from rice husk. *Industrial Crops and Products*, *37*(1), 93–99. http://doi.org/10.1016/J.INDCROP.2011.12.016

Kabir, M. M., Wang, H., Lau, K. T., & Cardona, F. (2013). Effects of chemical treatments on hemp fibre structure. *Applied Surface Science*, *276*, 13–23. http://doi.org/10.1016/J.APSUSC.2013.02.086

Kargarzadeh, H., Ahmad, I., Abdullah, I., Dufresne, A., Zainudin, S. Y., & Sheltami, R. M. (2012). Effects of hydrolysis conditions on the morphology, crystallinity, and thermal stability of cellulose nanocrystals extracted from kenaf bast fibers. *Cellulose*, *19*(3), 855–866. http://doi.org/10.1007/s10570-012-9684-6

Kargarzadeh, H., Huang, J., Lin, N., Ahmad, I., Mariano, M., Dufresne, A., … Gałęski, A. (2018). Recent developments in nanocellulose-based biodegradable polymers, thermoplastic polymers, and porous nanocomposites. *Progress in Polymer Science*. http://doi.org/10.1016/J.PROGPOLYMSCI.2018.07.008

Kasiri, N., & Fathi, M. (2018). Production of cellulose nanocrystals from pistachio shells and their application for stabilizing Pickering emulsions. *International Journal of Biological Macromolecules*, *106*, 1023–1031. http://doi.org/10.1016/J.IJBIOMAC.2017.08.112

Kennedy, M., List, D., Lu, Y., Foo, L. Y., Robertson, A., Newman, R. H., & Fenton, G. (1999). Kiwifruit Waste and Novel Products Made from Kiwifruit Waste: Uses, Composition and Analysis (pp. 121–152). Springer, Berlin, Heidelberg. http://doi.org/10.1007/978-3-662-03887-1_5

Kumar, A., Negi, Y. S., Choudhary, V., & Bhardwaj, N. K. (2014). Characterization of Cellulose Nanocrystals Produced by Acid-Hydrolysis from Sugarcane Bagasse as Agro-Waste. *Journal of Materials Physics and Chemistry*, *2*(1), 1–8. http://doi.org/10.12691/JMPC-2-1-1

Kvavadze, E., Bar-Yosef, O., Belfer-Cohen, A., Boaretto, E., Jakeli, N., Matskevich, Z., & Meshveliani, T. (2009). 30,000-year-old wild flax fibers. *Science (New York, N.Y.)*, *325*(5946), 1359. http://doi.org/10.1126/science.1175404

Lamaming, J., Hashim, R., Leh, C. P., Sulaiman, O., Sugimoto, T., & Nasir, M. (2015). Isolation and characterization of cellulose nanocrystals from parenchyma and vascular bundle of oil palm trunk (Elaeis guineensis). *Carbohydrate Polymers*, *134*, 534–540. http://doi.org/10.1016/j.carbpol.2015.08.017

Li, Y., & Pickering, K. L. (2008). Hemp fibre reinforced composites using chelator and enzyme treatments. *Composites Science and Technology*, *68*(15–16), 3293–3298. http://doi.org/10.1016/J.COMPSCITECH.2008.08.022

Lu, P., & Hsieh, Y.-L. (2010). Preparation and properties of cellulose nanocrystals: Rods, spheres, and network. *Carbohydrate Polymers*, *82*(2), 329–336.

http://doi.org/10.1016/J.CARBPOL.2010.04.073
Luzi, F., Fortunati, E., Giovanale, G., Mazzaglia, A., Torre, L., & Balestra, G. M. (2017). Cellulose nanocrystals from Actinidia deliciosa pruning residues combined with carvacrol in PVA_CH films with antioxidant/antimicrobial properties for packaging applications. *International Journal of Biological Macromolecules*, *104*, 43–55. http://doi.org/10.1016/j.ijbiomac.2017.05.176
Luzi, F., Fortunati, E., Jiménez, A., Puglia, D., Pezzolla, D., Gigliotti, G., … Torre, L. (2016). Production and characterization of PLA_PBS biodegradable blends reinforced with cellulose nanocrystals extracted from hemp fibres. *Industrial Crops and Products*, *93*, 276–289. http://doi.org/10.1016/J.INDCROP.2016.01.045
Luzi, F., Fortunati, E., Puglia, D., Lavorgna, M., Santulli, C., Kenny, J. M., & Torre, L. (2014). Optimized extraction of cellulose nanocrystals from pristine and carded hemp fibres. *Industrial Crops and Products*, *56*, 175–186. http://doi.org/10.1016/J.INDCROP.2014.03.006
Luzi, F., Fortunati, E., Puglia, D., Petrucci, R., Kenny, J. M., & Torre, L. (2016). Modulation of Acid Hydrolysis Reaction Time for the Extraction of Cellulose Nanocrystals from *Posidonia oceanica* Leaves. *Journal of Renewable Materials*, *4*(3), 190–198. http://doi.org/10.7569/JRM.2015.634134
Mandal, A., & Chakrabarty, D. (2011). Isolation of nanocellulose from waste sugarcane bagasse (SCB) and its characterization. *Carbohydrate Polymers*, *86*(3), 1291–1299. http://doi.org/10.1016/J.CARBPOL.2011.06.030
Mariano, M., El Kissi, N., & Dufresne, A. (2016). Cellulose nanocrystal reinforced oxidized natural rubber nanocomposites. *Carbohydrate Polymers*, *137*, 174–183. http://doi.org/10.1016/J.CARBPOL.2015.10.027
Matos Ruiz, M., Cavaillé, J. Y., Dufresne, A., Gérard, J. F., & Graillat, C. (2000). Processing and characterization of new thermoset nanocomposites based on cellulose whiskers. *Composite Interfaces*, *7*(2), 117–131. http://doi.org/10.1163/156855400300184271
Neus Anglès, M., & Dufresne, A. (2001). Plasticized Starch/Tunicin Whiskers Nanocomposite Materials. 2. Mechanical Behavior. *Macromolecules*, *34*(9), 2921–2931. http://doi.org/10.1021/MA001555H
Nguyen, T., Zavarin, E., & barrall, E. M. (1981). Thermal Analysis of Lignocellulosic Materials. *Journal of Macromolecular Science, Part C*, *20*(1), 1–65. http://doi.org/10.1080/00222358108080014
Novellino, D. (2007). Ampelodesmos mauritanicus - The role of Ampelodesmos mauritanicus and fibre plants in central Italy. *Non-Wood News*, *14*, 24–25.
Pelissari, F. M., Sobral, P. J. do A., & Menegalli, F. C. (2014). Isolation and characterization of cellulose nanofibers from banana peels. *Cellulose*, *21*(1), 417–432. http://doi.org/10.1007/s10570-013-0138-6
Puglia, D., Petrucci, R., Fortunati, E., Luzi, F., Kenny, J. M., & Torre, L. (2014). Revalorisation of Posidonia Oceanica as Reinforcement in Polyethylene/Maleic Anhydride Grafted Polyethylene Composites. *Journal of Renewable Materials*, *2*(1), 66–76. http://doi.org/10.7569/JRM.2013.634134
Sacui, I. A., Nieuwendaal, R. C., Burnett, D. J., Stranick, S. J., Jorfi, M., Weder, C., … Gilman, J. W. (2014). Comparison of the Properties of Cellulose Nanocrystals and Cellulose Nanofibrils Isolated from Bacteria, Tunicate, and Wood Processed Using Acid, Enzymatic, Mechanical, and Oxidative Methods. *ACS Applied Materials & Interfaces*, *6*(9), 6127–6138. http://doi.org/10.1021/am500359f
Sain, M., & Panthapulakkal, S. (2006). Bioprocess preparation of wheat straw fibers and their characterization. *Industrial Crops and Products*, *23*, 1–8.
Saliba, E. de O. S., Rodriguez, N. M., Morais, S. A. L. de, & Piló-Veloso, D. (2001). Ligninas: métodos de obtenção e caracterização química. *Ciência Rural*, *31*(5), 917–928. http://doi.org/10.1590/S0103-84782001000500031

Sheltami, R. M., Abdullah, I., Ahmad, I., Dufresne, A., & Kargarzadeh, H. (2012). Extraction of cellulose nanocrystals from mengkuang leaves (Pandanus tectorius). *Carbohydrate Polymers*, *88*(2), 772–779. http://doi.org/10.1016/J.CARBPOL.2012.01.062

Shi, Q., Zhou, C., Yue, Y., Guo, W., Wu, Y., & Wu, Q. (2012). Mechanical properties and in vitro degradation of electrospun bio-nanocomposite mats from PLA and cellulose nanocrystals. *Carbohydrate Polymers*, *90*(1), 301–308. http://doi.org/10.1016/J.CARBPOL.2012.05.042

Silvério, H. A., Flauzino Neto, W. P., Dantas, N. O., & Pasquini, D. (2013). Extraction and characterization of cellulose nanocrystals from corncob for application as reinforcing agent in nanocomposites. *Industrial Crops and Products*, *44*, 427–436. http://doi.org/10.1016/J.INDCROP.2012.10.014

Thambiraj, S., & Ravi Shankaran, D. (2017). Preparation and physicochemical characterization of cellulose nanocrystals from industrial waste cotton. *Applied Surface Science*, *412*, 405–416. http://doi.org/10.1016/J.APSUSC.2017.03.272

Thomas, D. W., & Owen, N. L. (1989). Infrared Studies of Hard and Soft Woods. *Applied Spectroscopy, Vol. 43, Issue 3, Pp. 451-455*, *43*(3), 451–455. Retrieved from https://www.osapublishing.org/as/abstract.cfm?uri=as-43-3-451

Toudert, N., Djilani, S. E., & Djilani, A. (2009). Antimicrobial activity of flavonoids of Ampelodesma mauritanica. *American-Eurasian Journal of Sustainable Agriculture*, 227–229. Retrieved from http://go.galegroup.com/ps/anonymous?id=GALE%7CA235407261&sid=googleScholar&v=2.1&it=r&linkaccess=abs&issn=19950748&p=AONE&sw=w

Toudert, N., Djilani, S. E., Djilani, E., Dicko, A., & Soulimani, R. (2009). Antimicrobial activity of the butanolic and methanolic extracts of Ampelodesma mauritanica. *Advances in Natural and Applied Sciences*, *3*(1), 19–21.

Yang, W., Fortunati, E., Luzi, F., Kenny, J. M., Torre, L., & Puglia, D. (2018). Lignocellulosic Based Bionanocomposites for Different Industrial Applications. *Current Organic Chemistry*, *22*(12), 1205–1221. http://doi.org/10.2174/1385272822666180515120948

Yu, H., Qin, Z., Liang, B., Liu, N., Zhou, Z., & Chen, L. (2013). Facile extraction of thermally stable cellulose nanocrystals with a high yield of 93% through hydrochloric acid hydrolysis under hydrothermal conditions. *Journal of Materials Chemistry A*, *1*(12), 3938. http://doi.org/10.1039/c3ta01150j

738 **Graphical Abstract**

739

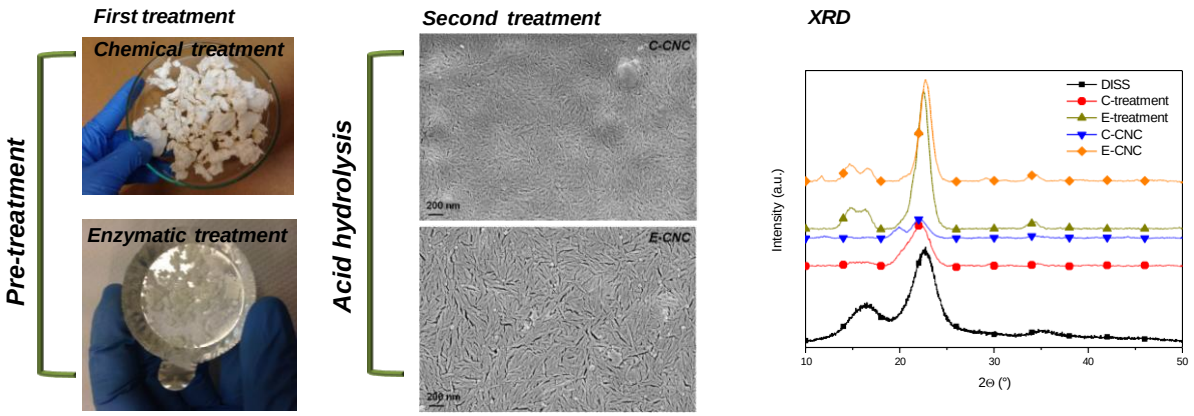

740